

Contribution of the east–west thermal heating contrast to the South Asian Monsoon and consequences for its variability

Fred Kucharski · Annalisa Bracco ·
Rondrotiana Barimalala · Jin Ho Yoo

Received: 19 January 2010/Accepted: 19 May 2010/Published online: 6 June 2010
© Springer-Verlag 2010

Abstract The focus of this paper is to assess the relative role of the north–south and east–west contrasts in atmospheric heating for the maintenance of the South Asian summer monsoon climatology. The juxtaposition of the Eurasian land mass and the Indian Ocean is responsible for the north–south contrast, while the greater diabatic heating above the western Pacific compared to the one over the African and the tropical South Atlantic Ocean region introduces the east–west gradient. With a series of idealized atmospheric general circulation model experiments, it is found that both contrasts contribute to the maintenance of the South Asian monsoon climatology, but their impact varies at regional scales. The surface atmospheric cyclone and precipitation over northern India are mainly due to the north–south contrast. On the other hand, when the Indian Ocean sea surface temperatures are close to their climatological mean values, the low-level cyclone and consequent rainfall activity in the Bay of Bengal and southern India result from the east–west gradient. The physical mechanism relays on the southern part of the upper-level South Asian monsoon high being forced by the east–west diabatic heating contrast via Sverdrup balance. The east–west heating difference controls also the strength of the Tropical Easterly Jet. Finally, the contribution of the El

Niño Southern Oscillation to the interannual variability of the Indian monsoon is interpreted as the result of a longitudinal shift of one of the centers of diabatic heating contributing to the east–west contrast.

Keywords South Asian Monsoon · SST forcing · Climate Variability · ENSO

1 Introduction

Monsoon systems are traditionally described as continental-scale 'sea-breeze' phenomena: in summer the smaller heat capacity of the land masses compared to that of the oceans leads to stronger surface warming over land compared to the ocean surfaces, which drives large-scale circulations. This involves low-level convergence and upper-level divergence over land, and the opposite over the oceans (e.g. Holton 1992; Wallace and Hobbs 1977, and references therein). When applied to South Asia this theory links the summer monsoon with the north–south contrast between the Eurasian land mass, and in particular the Tibetan Plateau, and the Indian Ocean (i.e. Webster 1987; Meehl 1994; Li and Yanai 1996 to cite a few). Chou (2003) further explored the effects of land-sea contrast modification on the Asian summer monsoon using idealized AGCM integrations and found that a strengthened meridional temperature gradient enhances the Asian summer monsoon, favoring strong convection. More recently Boos and Kuang (2010) suggested that the orographic insulation provided by the Himalayas and adjacent mountains is more important in determining the land–sea contrast than the Tibetan plateau heating per se.

On the other hand, Chao and Chen (2001) interpreted the monsoons as a 10° displacement of the intertropical

F. Kucharski (✉) · R. Barimalala · J. H. Yoo
Abdus Salam International Centre for Theoretical Physics,
Earth System Physics Section, Strada Costiera 11,
34151 Trieste, Italy
e-mail: kucharsk@ictp.it

A. Bracco
EAS, Georgia Institute of Technology, 311 First Dr,
Atlanta, GA 30332, USA

convergence zone (ITCZ) away from the equator. By replacing Asia, the maritime continent and Australia by ocean, and therefore removing the land–sea contrast, they showed with idealized numerical experiments that the western Pacific/Indian monsoon system would still exist with characteristics similar to those observed. The presence of warm sea surface temperatures (SSTs) in the Indo/Pacific basins and the tropical large-scale atmospheric circulation are sufficient to support low-level convergence. However, in these simulations the monsoon is not extending as far north as in the observations. In this scenario other large-scale circulation components, such as the upper-level monsoon high, are interpreted as a Gill-response (Gill 1980) to the atmospheric heating near the warmest SSTs. Thus in conclusion Chao and Chen (2001) suggest that land masses enhance the low-level convergence induced by the northward ITCZ displacement and cause a northward shift of the rainfall, but the land-sea contrast per se is not necessary to the existence of the Asian Monsoon system.

Recently, Chen (2003) proposed to revise the monsoon systems theory adopting a global prospective based on observational data. Focusing on the Asian Monsoon, the author indicates that the main driver is the east–west diabatic heating gradient between the western tropical Pacific and the African/Atlantic region. Analyzing the upper level streamfunction distribution, Chen (2003) indeed shows that the Tibetan high may be interpreted as the result of Sverdrup balance (e.g. Rodwell and Hoskins 2001) of the strong upper-level divergence–convergence contrast between the western tropical Pacific and the African/Atlantic region.

The aim of this paper is to further refine our understanding of the mechanisms proposed above. With a set of idealized atmospheric general circulation model (AGCM) experiments we demonstrate that both the north–south contrast, linked to the different thermal heating between land and ocean, and the east–west contrast, due to the differences in SSTs in the western Pacific warm pool versus the Atlantic basin, contribute to the observed characteristics of the Indian Monsoon. Furthermore, we discuss the relative role of the two contributions and the consequences for the monsoon interannual variability with particular focus on the El Niño Southern Oscillation (ENSO)—Indian Monsoon relationship. Changes in the Walker circulation associated with ENSO have a well established influence on the South Asian summer monsoon, with negative rainfall anomalies over India in the summer preceding peak El Niño conditions, and viceversa during the development of La Niña, (Walker 1924; Rasmusson and Carpenter 1983; Webster and Yang 1992; Ju and Slingo 1995; Goswamy 1998, Turner et al. 2007; Li et al. 2007 amongst others). However, the details of the physical

mechanisms proposed to explain the ENSO influence on the Indian monsoon are rather complex. Here we show that changes in the east–west contrast outside the Indian Ocean region, similar to those resulting from the ENSO activity, can lead to large variations of the South Asian monsoon strength.

We present the model and experimental set-up in Sect. 2, followed by the results in Sect. 3. Discussion and conclusions are given in Sect. 4.

2 Model, experimental design and data used

The model adopted in this study is the International Centre for Theoretical Physics (ICTP) AGCM (Molteni 2003). It is based on a hydrostatic spectral dynamical core (see Held and Suarez 1994), and uses the vorticity-divergence form described by Bourke (1974). The parameterized processes include short- and long-wave radiation, large-scale condensation, convection, surface fluxes of momentum, heat and moisture, and vertical diffusion. Convection is represented by a mass-flux scheme that is activated where conditional instability is present, and boundary layer fluxes are obtained by stability-dependent bulk formulae. Land and ice temperature anomalies are determined by a simple one-layer thermodynamic model. In this study the AGCM is configured with eight vertical (sigma) levels and with a spectral truncation at total wavenumber 30. Applications of the ICTP AGCM can be found in e.g. Bracco et al. (2004); Kucharski et al. (2006a, 2006b, 2009a).

We conduct six experiments:

- CNTRL: a 50-year long control integration with the ICTP AGCM forced by monthly varying climatological SSTs.
- ZONAL: a 50-year sensitivity integration where climatological SSTs are replaced by their zonal mean values everywhere except in the Indian Ocean (30°E to 110°E).
- ZONAL_{NoCon}: a 50-year long integration where climatological SSTs are replaced by their zonal mean values everywhere except in the Indian Ocean and all continents apart from the Asian land-mass are removed. SSTs set to their zonal mean values replace the continents.
- ZONAL_{Pac}: a 50-year integration where climatological SSTs are replaced by their zonal mean values only in the Pacific basin.
- ZONAL_{Atl}: a 50-year integration where climatological SSTs are replaced by their zonal mean values only in the Atlantic basin.
- ALBEDO: a 50-year integration forced by climatological SSTs with the albedo over the South Asian longitudes

(45°E to 115°E, 15°N to 90°N) increased by 50% compared to standard values.

ZONAL allows to investigate the impact of SST deviations from their zonal mean outside the Indian Ocean region; ZONAL_{Pac} and ZONAL_{Atl} focus on the respective role of SST deviations on the Pacific and Atlantic oceans and are used to better interpret the outcome of the ZONAL experiment; ZONAL_{NoCon} lets us study the monsoon system in the absence of any east–west heating contrast outside the Indian region; and ALBEDO focuses on the north–south contrast and on how its variations can modify the Asian monsoon.

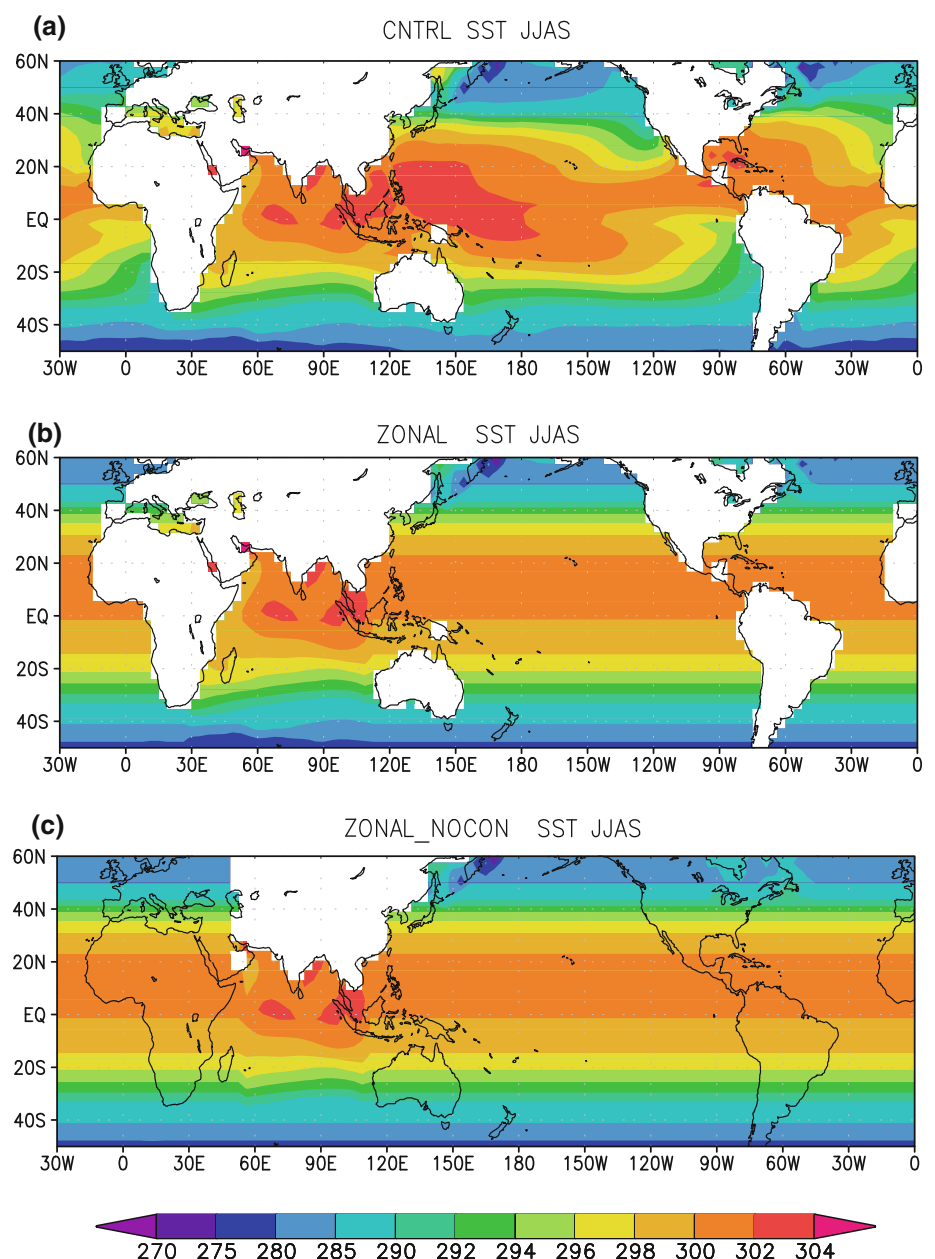
Figure 1a–c show the SST and land-sea mask (white area for land) distributions in the experiments CNTRL,

ZONAL and ZONAL_{NoCon}, respectively, whereas Fig. 2 shows the albedo distributions of the experiments CNTRL and ALBEDO, the corresponding temperature responses and their differences.

The SSTs in the Indian Ocean region are set to climatological values in all runs. This is done to better compare results from the different integrations with the control one and to avoid that local SST changes in the Indian monsoon area may influence the outcome of our investigation.

In the following we will present climatological fields averaged from June to September (JJAS season) from the various experiments and deviations of ZONAL, ZONAL_{NoCon}, and ALBEDO from the control. All

Fig. 1 SST and land/sea distribution in the different experiments: **a** CNTRL, **b** ZONAL, **c** ZONAL_{NoCon}. Land areas are indicated by the white colour. Units are K



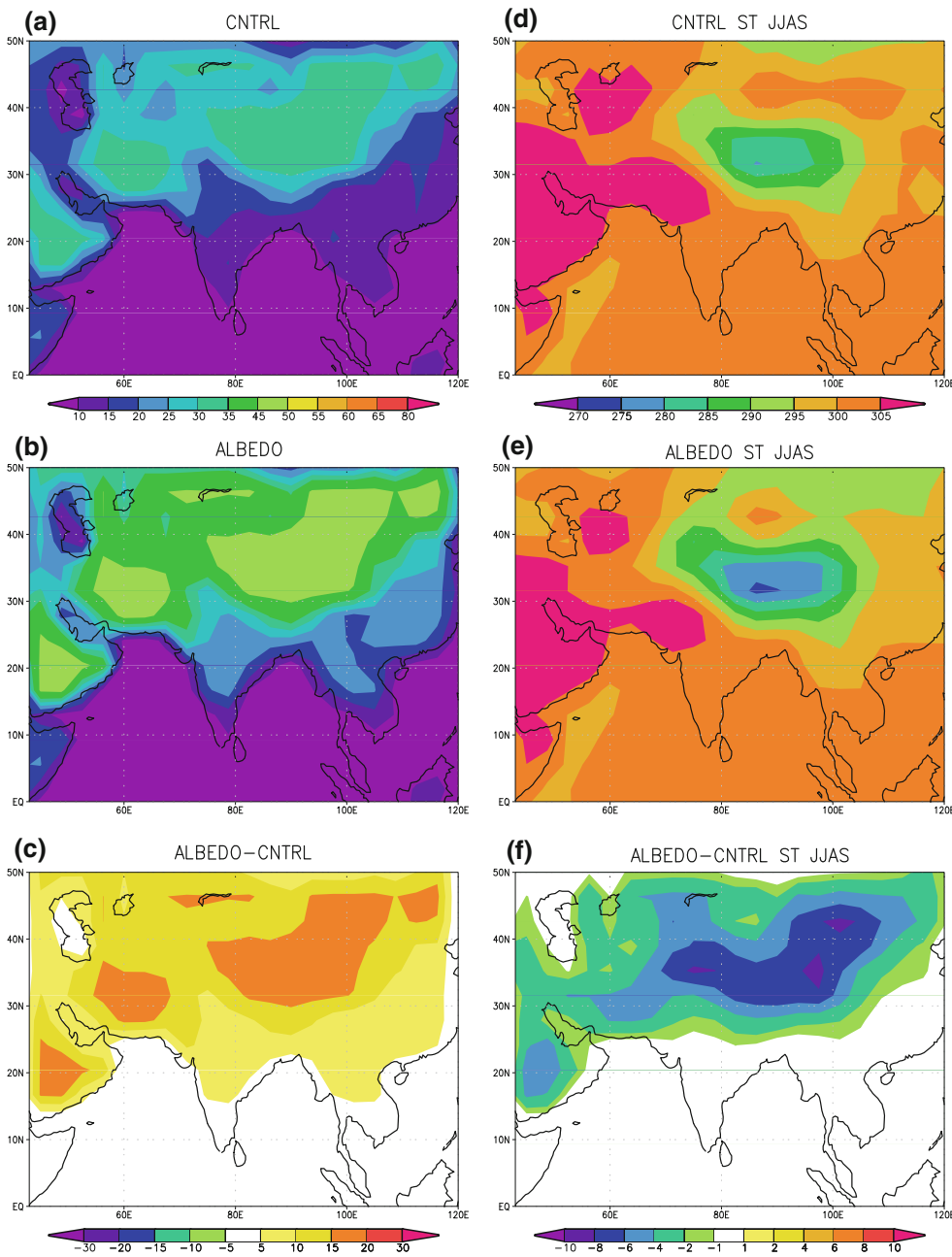


Fig. 2 Albedo and Surface temperature in **a, d)** CNTRL, **b, e)** ALBEDO experiments, **c, f)** their differences. Units are % in **a–c** and K in **d–f**

deviations shaded in the figures are 95% statistically significant according to a *t* test under the assumption of 50 independent records of seasonal means.

When diagnosing the interannual variability of the South Asian monsoon linked to changes in tropical Pacific SSTs, we also consider a 10-member ensemble performed for the CLIVAR International ‘Climate of the 20th Century’ (C20C) project (Folland et al. 2002; Scaife et al. 2009; Kucharski et al. 2009b). These integrations cover the period 1950–2002 and are forced with monthly varying SSTs

from the HadISST data set (Rayner et al. 2003) in the tropical Pacific region (130°E to the coast of South and Central America, 20°S to 20°N), and with climatological monthly varying SSTs elsewhere. We will refer to these integrations as C20C in the following. Table 1 summarizes the experiments and their purpose.

Comparisons with observations are performed using products from the NCEP/NCAR re-analysis (Kalnay et al. 1996), and rainfall data-sets from the Climate Prediction Merged Analysis of Precipitation (CMAP; Xie and Arkin

Table 1 Experiments used in this paper and their purpose

Experiment	SST	Land–sea mask	Purpose
CNTL	Climatological	Observed	Control experiment
ZONAL	Zonal outside Ind Ocean	Observed	Infl. of zonal SST asymm.
ZONAL _{NoCon}	Zonal outside Ind Ocean	Only Asia	Infl. of SST plus zonal land-sea asymm.
ZONAL _{Pac}	Zonal in Pacific	Observed	Infl. of zonal SST asymm. in Pac.
ZONAL _{Atl}	Zonal in Atlantic	Observed	Infl. of zonal SST asymm. in Atl.
ALBEDO	Climatological	Observed	Infl. of heating change over land
C20C	Monthly varying in trop Pac.	Observed	Trop. Pac. SST forcing

1997) and Global Precipitation Climatology Project (GPCP; Adler et al. 2003). In the following, all NCEP and model fields are evaluated from 1950 to 2002, while CMAP and GPCP precipitation data are available only from 1980 onward.

3 Results

3.1 Model climatology

Before analyzing the sensitivity experiments, it is useful to compare the model climatology with observations. Figure 3 displays in panel (a) the precipitation climatology with superimposed low-level 925 hPa winds for CMAP and NCEP/NCAR re-analysis respectively, and in panel (b) for the model. Overall, the ICTP AGCM captures the features of observed summer precipitation patterns and associated circulations quite well. Figure 4a, b focus the South Asian monsoon region. The model shows a cross-equatorial flow, the Somali Jet, even though weaker than observed, and precipitation maxima in the Bay of Bengal, over Northern India and over the equatorial and south-equatorial Indian Ocean. The precipitation maxima over the ocean coincide with the centers of the warmest SSTs in the Indian Ocean (one in the Bay of Bengal, the other in the equatorial and south-equatorial Indian Ocean) and generally overestimate the observed signal. The rainfall over large parts of the Indian peninsula, on the other hand, is underestimated. This bias is likely related to anomalous low-level divergence over northern India in the model. These model biases, typical of most AGCM, have been attributed to several causes, ranging from low horizontal and/or vertical resolution to deficiencies in the convection and surface-flux parameterizations. We have found that the lack of interactive air-sea coupling in the Indian Ocean/Western Pacific region is one of the major sources of errors and Bracco et al. (2007) discussed the improvements in the climatology obtained by choosing a regional coupling strategy, in agreement with other studies (e.g. Wang et al. 2005; Wu and Kirtman 2005). Nevertheless, in this work we opted for simpler AGCM integrations instead of a

regionally coupled set-up given the highly idealized nature of the experiments performed. It would be indeed difficult to control changes in heating contrast with a coupled model. By comparing the climatologies of the sensitivity experiments with the control run we hope to infer meaningful information in spite of model biases.

Figure 5 shows the Tropical Easterly Jet (TEJ) as measured by the 200 hPa zonal wind. The TEJ is an integral part of the Asian monsoon system. Both observations (5a) and the model (5b) display the TEJ centered with its maximum in the Indian Ocean region, extending into Africa to the west and to the Pacific warm pool to the east, even though the TEJ of the model is weaker than observed.

Finally, the climatological fields of 200 hPa velocity potential and 200 hPa eddy stream function are shown in Fig. 6a, b with the model counterparts from CNTL in panels (c) and (d), respectively. The ICTP AGCM reproduces fairly well the main global features of the South Asian monsoon, with the velocity potential minimum corresponding to upper-level divergence located just over the western Pacific warm pool region, whereas the maximum, i.e. upper-level convergence, is located over Africa, the South Atlantic Ocean and South America. The modeled velocity potential minimum does not extend far enough into the eastern Pacific region. The upper-level eddy streamfunction is in quadrature with the velocity potential. This implies, for example, that the South Asian monsoon high, corresponding to the streamfunction maximum, lies just in the gradient of the velocity potential and results from Sverdrup balance as described by Eq. 5 in Chen (2003). The position and strength of the South Asian monsoon high, also known as Tibetan high, are crucial to the South Asian monsoon (e.g. Chen 2003) and are well reproduced by the AGCM. The modeled eddy streamfunction response of Fig. 6d, however, is not extending far enough into the north African region. This bias is consistent with a more intense than observed velocity potential over Africa.

3.2 Sensitivity experiments

Having described the model climatology, we now investigate the sensitivity experiments. Figure 7 displays the

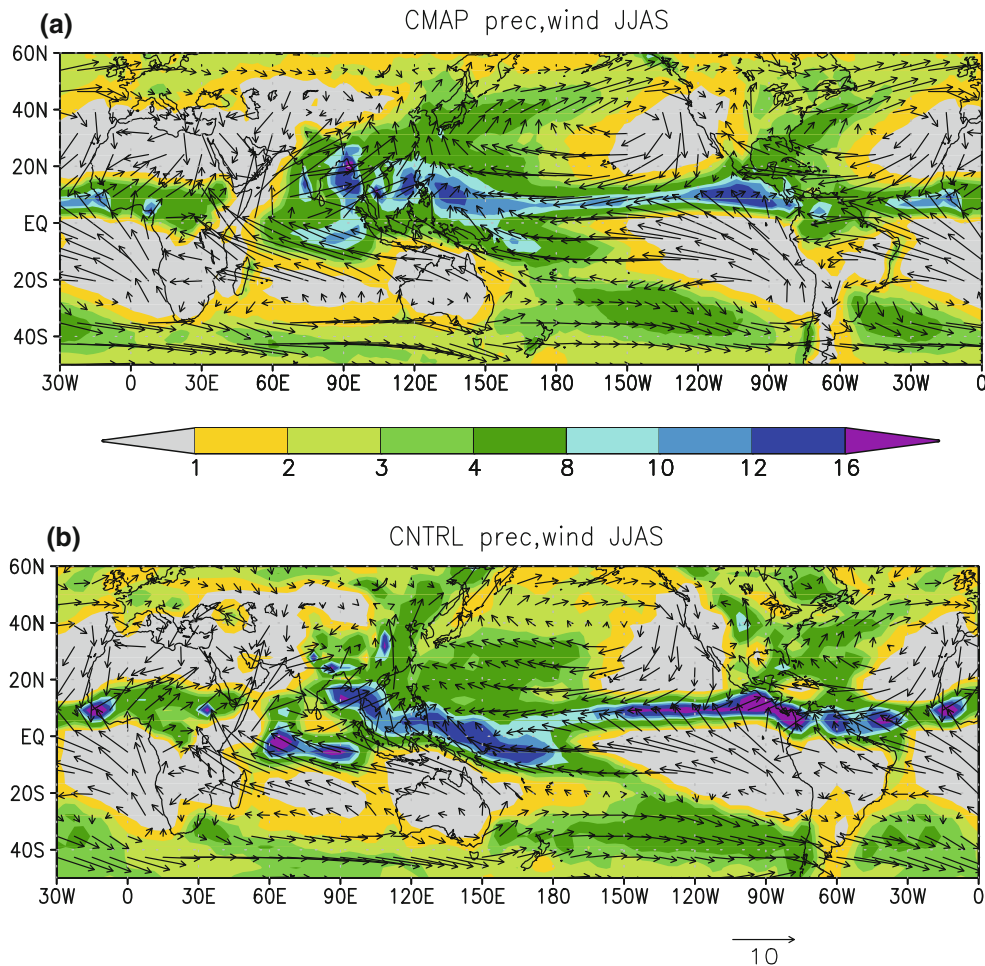


Fig. 3 **a** Observed (CMAP, NCEP) and **b** modeled (CNTRL) precipitation and 925 hPa wind climatologies. Units are mm/day for precipitation and m/s for wind

global precipitation distributions for ZONAL, ZONAL_{NoCon} and ALBEDO (left panels) and the relative changes with respect to the control simulation (right). The rainfall differences represent the response to the redistribution of global diabatic heating following the variations of local SSTs and land-masses. In the Indian Ocean basin the monsoonal changes are remotely forced, as a consequence of identical climatological SSTs being used in all runs. ZONAL and ZONAL_{NoCon} show similar and zonally symmetric precipitation distributions. Differences between those two runs are evident in the Atlantic basin, due to its limited lateral extension at the Tropics and to the presence of the South American and African land masses. ZONAL_{NoCon} is characterized by consistently zonally symmetric precipitation patterns everywhere, except for the Indian Ocean. ALBEDO, on the other hand, differs from CNTRL predominantly over South Asia and in the equatorial Indian Ocean, with more limited, but non-zero, changes over the other oceans and increased rainfall in south-east Europe. The rainfall response zoomed in the

South Asian monsoon region is presented in Fig. 8 together with the 925 hPa winds. Both ZONAL and ZONAL_{NoCon} display a substantial reduction of precipitation in the Bay of Bengal that appears as nearly dry. Such a reduction extends well into the Indochina peninsula and over central and southern India, while a significant increase in rainfall is observed over the equatorial Indian Ocean. Those features are enhanced when continents are replaced by zonally averaged SSTs. Furthermore, a weakened Somali jet characterizes the response. In ZONAL the north-western part of the jet is still recognizable and there is flow convergence in the northern Indian region. In ZONAL_{NoCon} regional circulation patterns lead to substantial convergence and precipitation in north-east India—even increased with respect to CNTRL—despite the overall weakened jet. The precipitation further north over the South Asian land mass is less influenced by the zonally averaged SSTs in the Pacific and Atlantic Oceans and shows little changes. Furthermore, over north-west India rainfall persists due to low-level convergence.

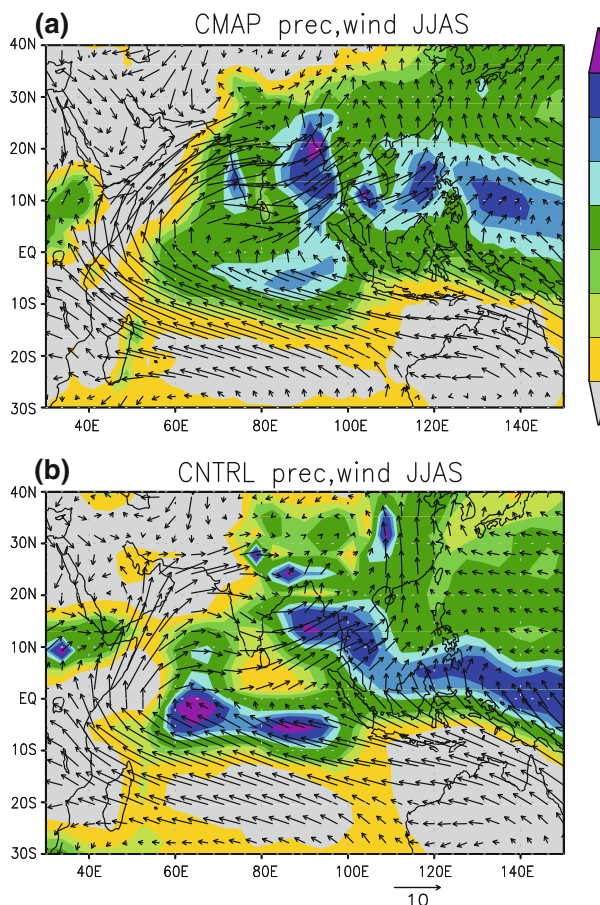


Fig. 4 **a** Observed (CMAP, NCEP) and **b** modeled (CNTRL) precipitation and 925 hPa wind climatologies. Units are mm/day for precipitation and m/s for wind

Higher albedo, and therefore lower temperatures over Asia (ALBEDO run), causes a band of increased rainfall centered around 7°N. Such a band extends from the western Indian Ocean into the southern portion of Indochina. Increased precipitation is also found over the north–west portion of India. North–East India, Bangladesh, the Tibetan Plateau and the northern part of the Indochina peninsula are significantly drier than in the CNTRL run. The role of the north–south contrast has been investigated with an alternative experiment in which all orographic features in Asia, including both the Himalayas and the Tibetan plateau, have been reduced to 300m elevation. The resulting precipitation patterns are strikingly similar to the ALBEDO case (not shown), indicating that the orography acts to increase and constrain the heating at high elevation, strengthening in turn the Tibetan high.

The outcome of these experiments suggests that the east–west thermal heating outside the Indian Ocean region, reduced in ZONAL and removed in ZONAL_{NoCon}, is altering substantially the rainfall amount near the two centers of maximum SSTs, the Bay of Bengal and the

equatorial Indian Ocean. Indeed, the east–west contrast appears to be responsible for the Bay of Bengal precipitation maximum and for the precipitation over southern India and Indochina. In the absence of the east–west contrast the rainfall preferentially resides over the southern maximum in the equatorial Indian Ocean causing a consistent decrease in the 10°N–20°N band. On the other hand, the north–south heating contrast induced by the Asian continent is responsible for the rainfall over the more continental areas of South Asia north of 13°N. To provide a more quantitative measure of the responses in the different experiments we calculated the average precipitation in the South Asian region (60°E–100°E, 10°N–25°N). The total average rainfall in the control simulation is 5.6 mm/day. The responses in ZONAL, ZONAL_{NoCon} and ALBEDO are –2.8, –3.6 and –1 mm/day, respectively. This shows that the contribution of the east–west contrast dominates the South Asian rainfall climatology.

The strong impact of the east–west heating contrast on the South Asian monsoon is further highlighted by the 200 hPa velocity potentials (Fig. 9) and streamfunctions (Fig. 10) of the various sensitivity experiments and by their differences with respect to CNTRL. Indeed, whenever zonal SSTs are prescribed over the Pacific and Atlantic oceans no velocity potential maximum forms in the Western Pacific, whereas ALBEDO displays velocity potential patterns consistent with the CNTRL experiment in the Western Pacific–African region, with the largest differences concentrated over the Indian basin. Consistently, in correspondence with the South Asian monsoon high, the upper-level streamfunction maximum from 10° to 30°N is strongly reduced in ZONAL and ZONAL_{NoCon} following Sverdrup balance, while is only weakly affected further North. This suggests that the southern part of the South Asian monsoon high is strongly influenced by the east–west heating contrast, whereas the northern component is mainly affected by the north–south contrast induced by the land-sea distributions. Our interpretation is confirmed by the analysis of the 200 hPa zonal velocity in the three integrations (Fig. 11). The TEJ weakens considerably in the first two experiments and less so in ALBEDO, indicating that a substantial part of its strength is due to the east–west heating contrast, with a more limited, although still statistically significant, contribution from the land-sea gradient.

To quantify the relative contributions of the Atlantic and the Pacific basins to the responses of experiment ZONAL, we performed two additional sensitivity experiments where only the Pacific SSTs (ZONAL_{Pac}) or the Atlantic SSTs (ZONAL_{Ait}) are set to their zonal mean climatological values. The resulting rainfall and wind changes are similar in structure to ZONAL, but with weaker amplitude (not shown). The area averaged precipitation changes in the

Fig. 5 **a** Observed (NCEP) and **b** modeled (CNTRL) 200 hPa wind climatology. Units are m/s

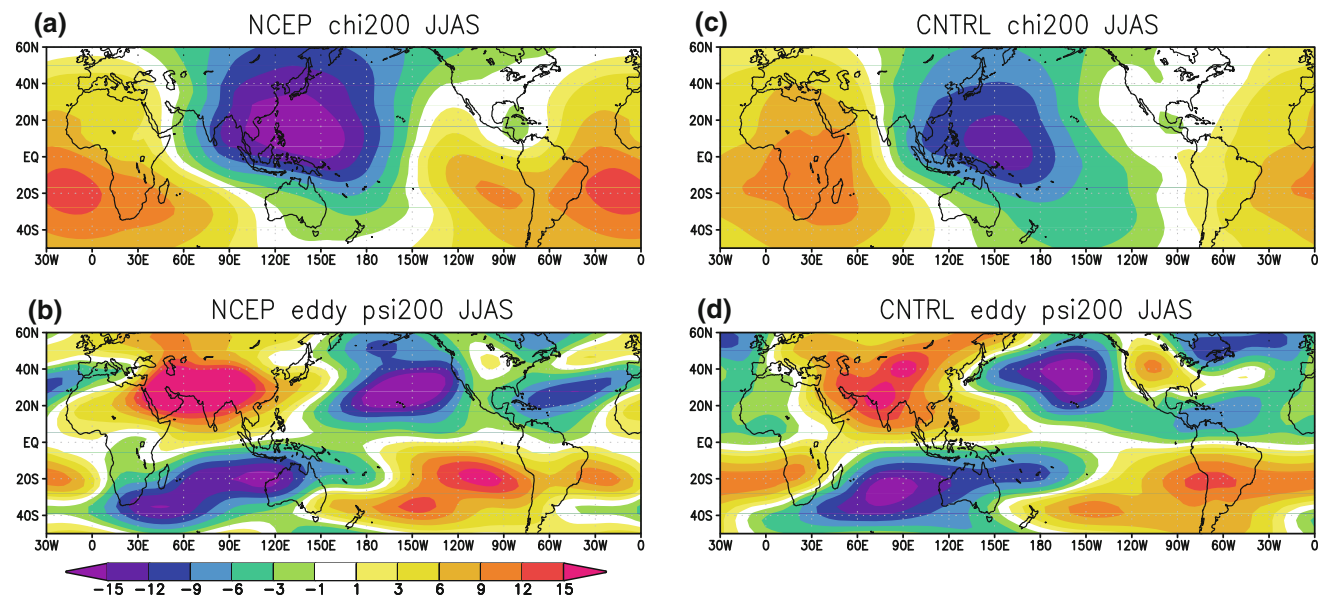
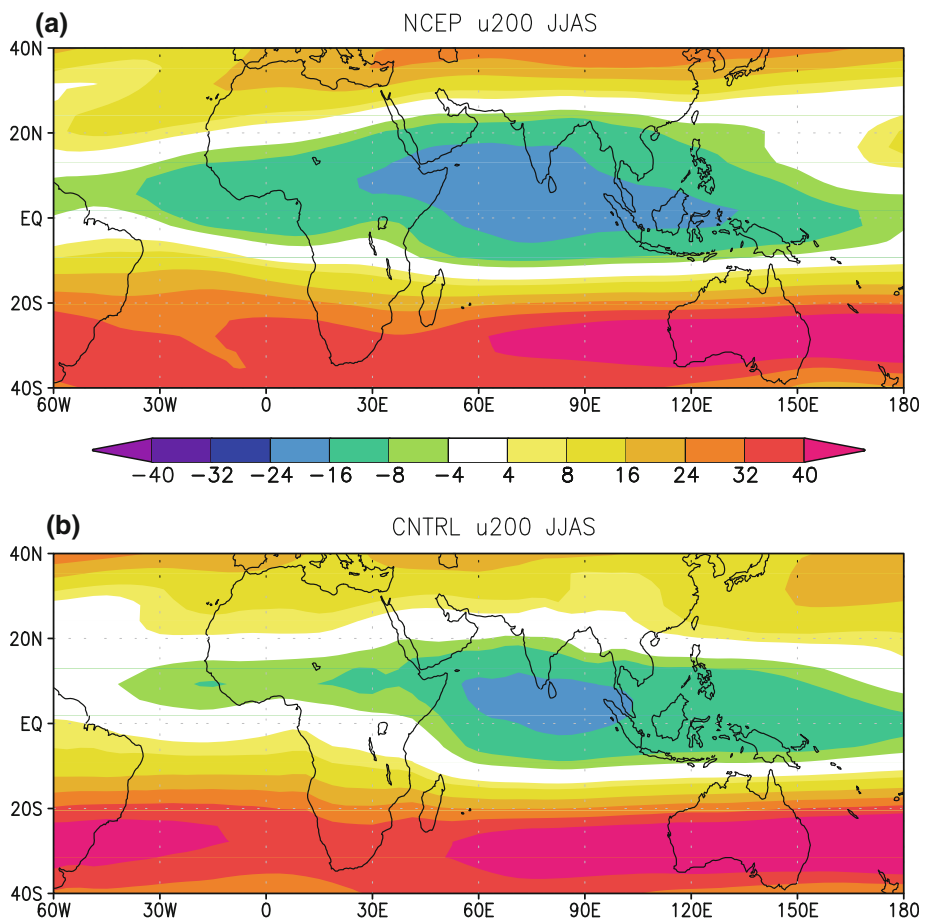


Fig. 6 Climatologies of 200 hPa velocity potential **a** NCEP, **c** CNTRL and 200 hPa eddy stream function **b** NCEP, **d** CNTRL. Units are $10^6 \text{m}^2/\text{s}$

South Asian region are -2.1 mm/day in the $\text{ZONAL}_{\text{Pac}}$ run and -1.3 mm/day for $\text{ZONAL}_{\text{Atl}}$. The relative size of the two basins, the larger east–west SST gradient in the

Pacific than in the Atlantic ocean, and the presence of Africa all contribute towards explaining the larger variation in $\text{ZONAL}_{\text{Pac}}$ compared to $\text{ZONAL}_{\text{Atl}}$. Additionally, the

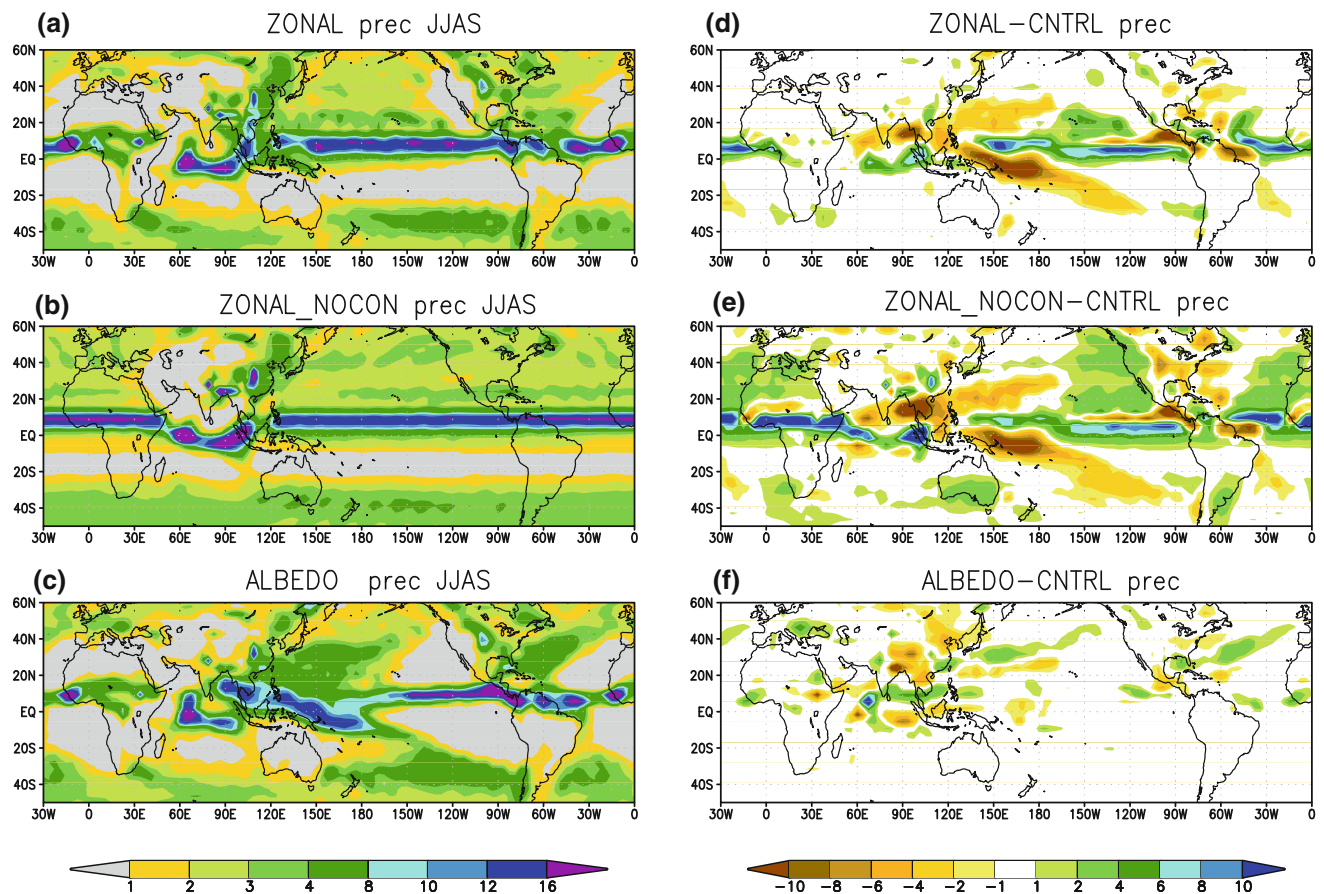


Fig. 7 Global precipitation in **a** ZONAL, **b** ZONAL_{NoCon}, **c** ALBEDO and the differences **d** ZONAL-CNTRL, **e** ZONAL_{NoCon}-CNTRL, **f** ALBEDO-CNTRL. Units are mm/day

sum of ZONAL_{Pac} and ZONAL_{Atl} contributions is different from ZONAL and this is indicative of nonlinear interactions.

3.3 Relevance for tropical SST forcings

By performing idealized studies on the relative contributions of the north–south and east–west heating contrast to the South Asian monsoon circulation, we have shown that the east–west gradient contributes significantly to the monsoon climatology. The east–west contrast is linked to the position and strength of the Walker circulation. It has been previously proposed that ENSO influences the South Asian monsoon by modifying the Walker circulation (Webster and Yang 1992; Ju and Slingo 1995; Wang 2006, amongst others). Here, we revisit this hypothesis in light of the results presented so far.

To investigate the ENSO impact on the South Asian monsoon we consider an ensemble of ten C20C simulations performed with the ICTP AGCM. Figure 12 shows the regression of observed (12a) and modeled (C20C; 12b)

200 hPa velocity potential onto the Niño3.4 index. Only anomalies that are statistically significant at the 90% confidence level are shown. Both observed and modeled regression maps indicate a distinct response in the velocity potential that is consistent with upper-level divergence in the eastern Pacific and upper-level convergence in the Indian Ocean region. Thus, such a response does not project strongly onto the structure of the time-mean velocity potential field, but indicates an eastward shift instead. This is further supported by the regression of the eddy 200 hPa streamfunction for both observations (Fig. 12c) and the model (Fig. 12d). A positive upper-level ridge response appears in the Central- to West Pacific, whereas a trough response is seen over Africa, again suggesting an eastward shift of the climatological mean streamfunction distribution. An opposite response characterizes the negative phase of ENSO or La Niña events. To our knowledge, and despite the vast literature on the ENSO-Indian monsoon relation, the ENSO-monsoon teleconnection has not yet been interpreted as resulting from a simple zonal shift of the east–west heating contrast. In agreement with our

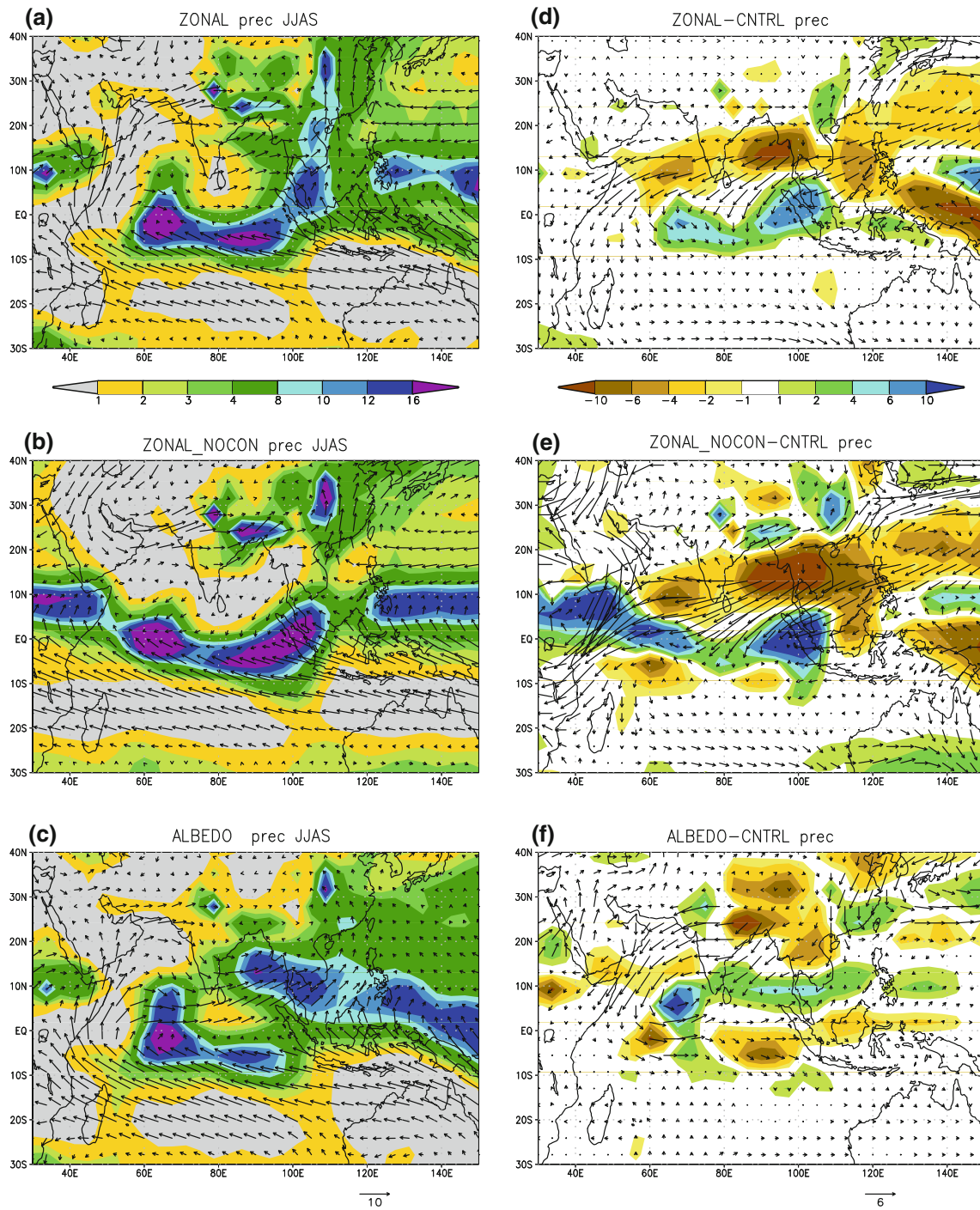


Fig. 8 South Asian precipitation and 925 hPa wind in **a** ZONAL, **b** ZONAL_{NoCon}, **c** ALBEDO and the differences **d** ZONAL-CNTRL, **e** ZONAL_{NoCon}-CNTRL, **f** ALBEDO-CNTRL. Units are mm/day for precipitation and m/s for wind

interpretation, recent studies (e.g. Annamalai et al. 2007 and Turner et al. 2005) have shown that only models which correctly position the diabatic heating anomalies associated with El Niño warming can simulate the correct ENSO-Indian monsoon teleconnection pattern.

Considering the rainfall climatology (Fig. 3), an eastward shift of the diabatic heating anomalies in the Pacific

during El Niños events would imply a tendency for a negative rainfall anomaly over the Indian Region, and vice-versa during La Niñas, given the gradient of precipitation in the region. Figure 13a–c show the regressions of rainfall onto the Nino3.4 index for GPCP and CMAP data set, and for the C20C ensemble mean, respectively. The observational data sets are available only after 1980, therefore our

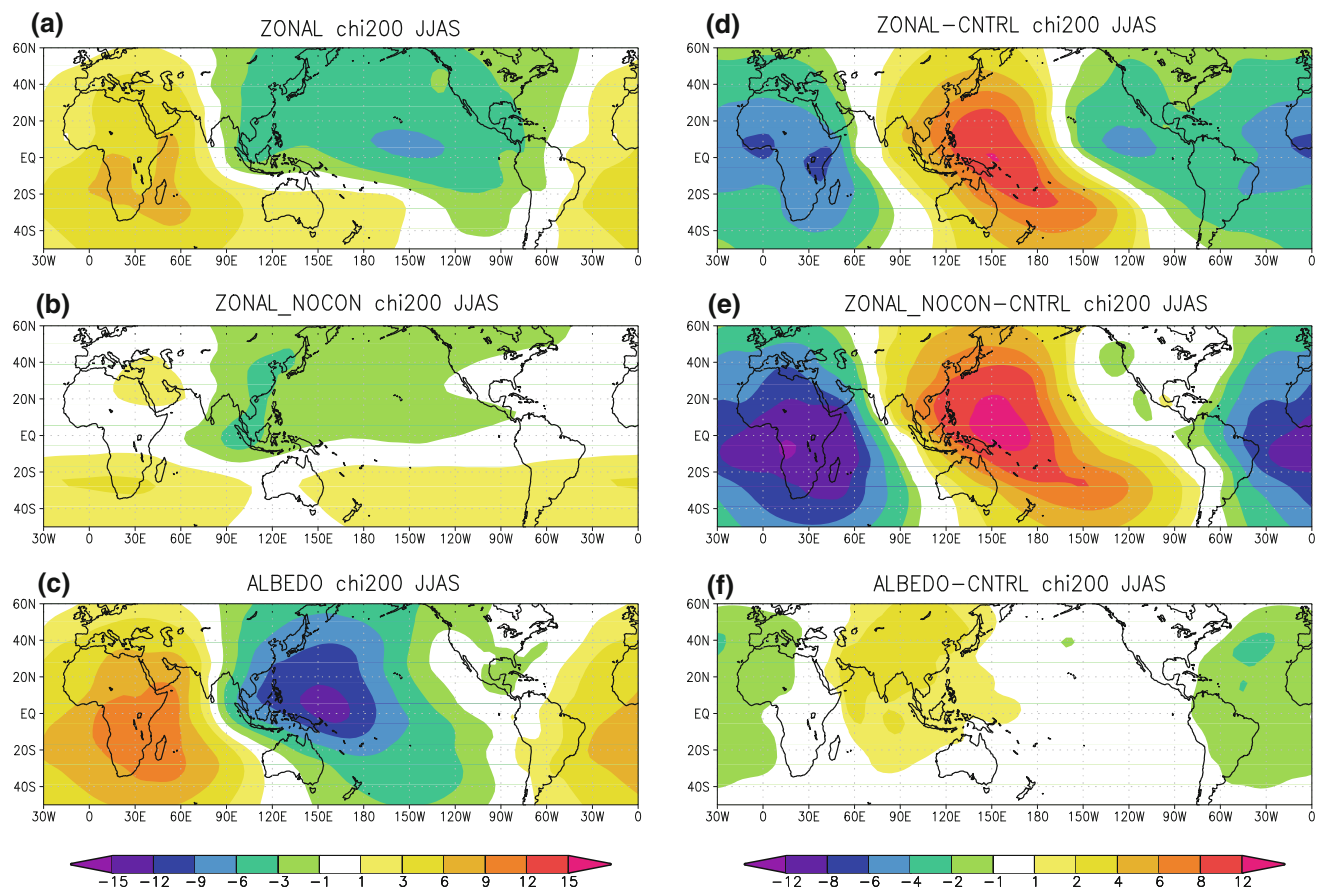


Fig. 9 Global velocity potential in **a** ZONAL, **b** ZONAL_{NoCon}, **c** ALBEDO and the differences **d** ZONAL–CNTRL, **e** ZONAL_{NoCon}–CNTRL, **f** ALBEDO–CNTRL. Units are $10^6 \text{ m}^2/\text{s}$

analysis is focused on the 1980–2002 period. Both GPCP and CMAP show an east–west precipitation dipole in the region 70°E to 120°E , 10°N to 25°N , with decreased rainfall to the west and increased rainfall to the east. In the model the increase in the eastern part is shifted by 5° – 10° to the south and is more pronounced than the decrease in the west. Furthermore, in the region 90°E to 130°E there is a pronounced north–south dipole structure in precipitation in the C20C ensemble. This feature is much weaker in the observations. It has been extensively documented that the ENSO–monsoon relationship is generally not well modeled in AGCM simulations that are forced by observed SSTs and that are not coupled in the Indian Ocean region (Krishna Kumar et al. 2005; Bracco et al. 2007; Kucharski et al. 2009b), and the ICTP AGCM is no exception. Coupled air-sea interactions in the Indian Ocean region likely play an important role in this relationship, and they are not taken into account in the AMIP-type set-up employed here. However, the model is capable of reproducing the upper-level responses quite well, and the precipitation response is indicative of the expected east–west dipole and relative

movement. Therefore, we suggest that part of the ENSO influence on the South Asian monsoon rainfall can be understood as driven by the eastward (westward) shift of the velocity potential and streamfunction centres during warm (cold) events.

SSTs in the South Tropical Atlantic are responsible for another externally forced component of the South Asian monsoon interannual variability, as found and extensively analyzed in the last few years (Kucharski et al. 2007, 2008, 2009a; Losada et al. 2009). The impact of the atmospheric teleconnection from Tropical Atlantic into the Indian Ocean is weaker than the ENSO signal, and is therefore difficult to completely separate from the ENSO influence in the short observational record of rainfall. Many idealized AGCM studies, however, have shown that the response from the Tropical Atlantic projects on the time-mean monsoon circulation causing reduced (increase) rainfall over South Asia for warm (cold) Atlantic SST anomalies. Such a response is not surprising in the framework proposed above, given that the relatively cold South Tropical Atlantic controls the western part of the east–west heating

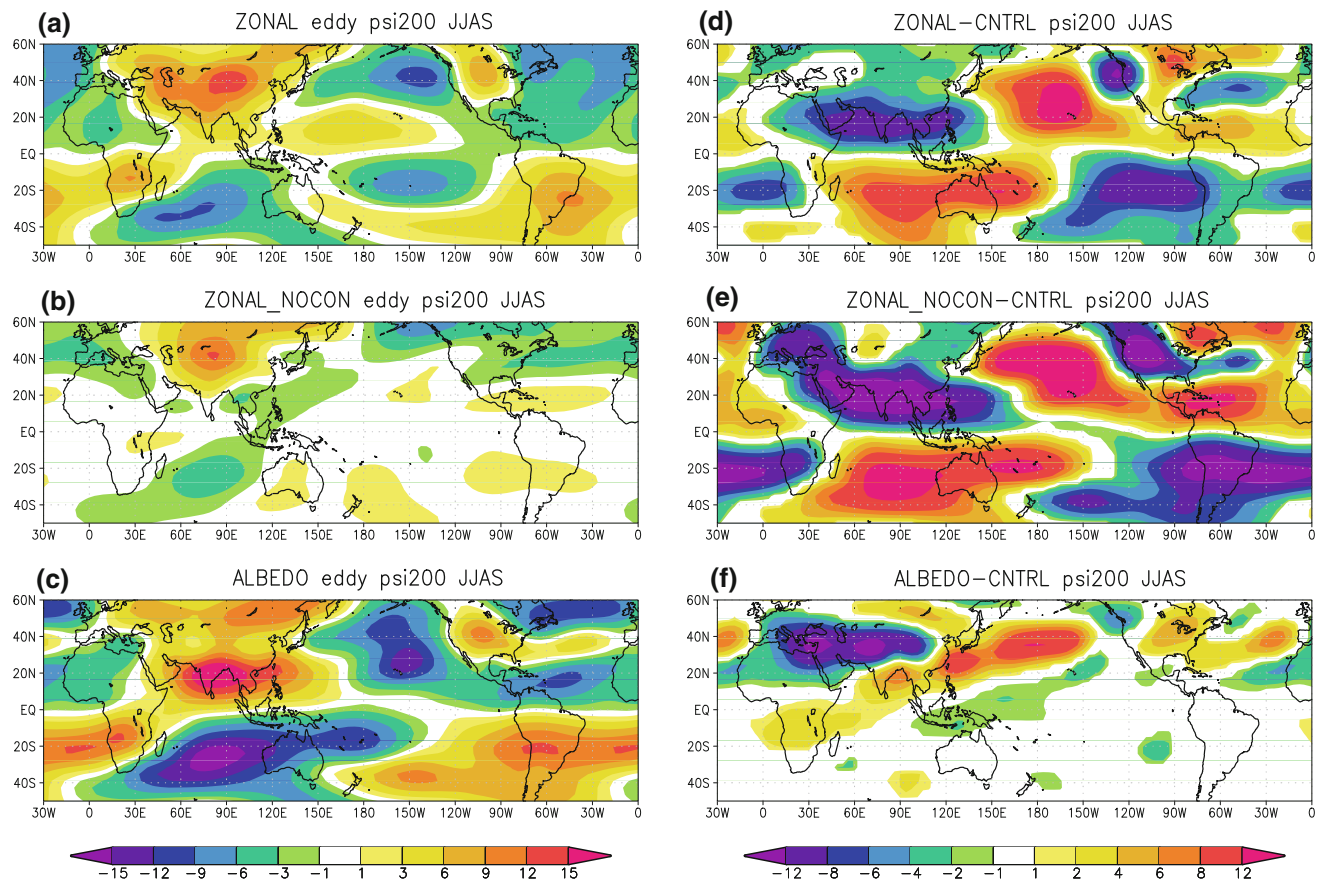


Fig. 10 Global eddy streamfunction in **a** ZONAL, **b** ZONAL_{NoCon}, **c** ALBEDO and the differences **d** ZONAL–CNTRL, **e** ZONAL_{NoCon}–CNTRL, **f** ALBEDO–CNTRL. Units are $10^6 \text{m}^2/\text{s}$

contrast, responsible for a large component of the South Asian monsoon trough, and that warm (cold) anomalies weakens (strengthens) the contrast. In this case the east–west gradient changes in amplitude but does not shift and the response projects directly onto the structure of the time mean velocity potential field and accordingly we found a substantial influence on South Asian rainfall in the experiment ZONAL_{Alt}, as discussed in Sect. 3.2.

4 Discussion and Conclusions

In this paper idealized AGCM experiments have been performed to investigate the relative role of the north–south (land-sea) and of the east–west contrasts in the mean heating on the South Asian monsoon climatology. We find that the diabatic heating maximum in the west Pacific, together with the minimum over Africa and the tropical Atlantic Ocean, force an upper-level eddy streamfunction maximum over the Indian region that may be interpreted as the southern part of the South Asian monsoon high.

Whereas the east–west heating contrast is mainly responsible for the rainfall maximum in the Bay of Bengal and for the precipitation over southern India, the north–south contrast induced by the land-sea distribution is responsible for the rainfall climatology further inland in the northern parts of India. Additionally, the east–west heating contrast modulates a large component of the Tropical Easterly Jet particularly in the Indian Ocean region and along the African coast.

This analysis is consistent with the interpretation of a Sverdrup balanced forcing of the southern part of the South Asian monsoon high by the east–west heating contrast and of the northern part by the land-sea contrast. These results confirm and refine the proposed global view of monsoon systems by Chen (2003).

Furthermore, we have shown that the ENSO-forced signal in upper-level velocity potential and streamfunction does not have the same structure of the climatological field. Instead, the regions of maximum ENSO-responses are in the eastern Pacific and Indian Ocean region, where the largest gradients in the climatological velocity potential are

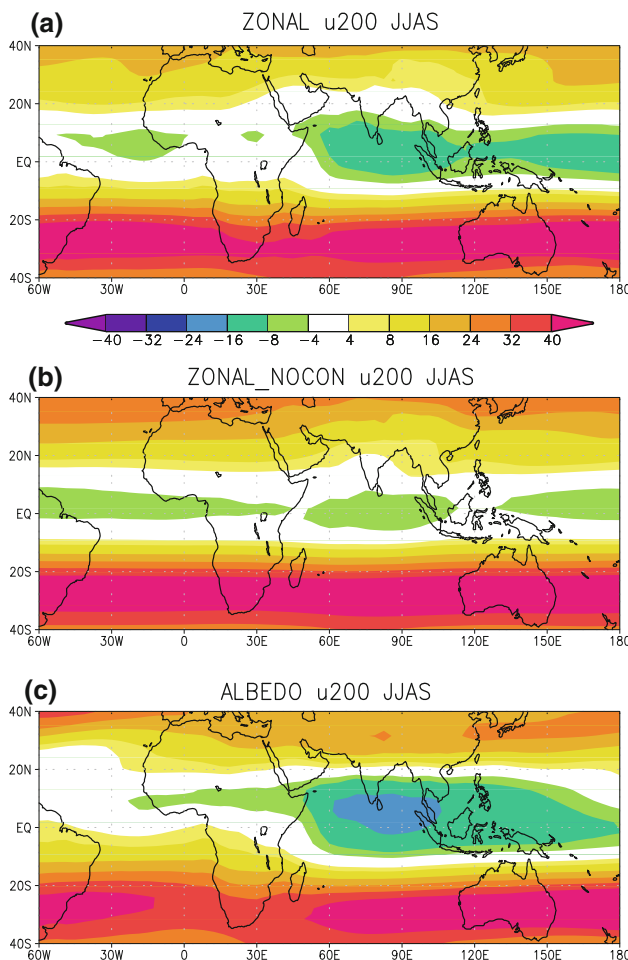


Fig. 11 200 hPa zonal wind in **a** ZONAL, **b** ZONAL_{NoCon}, **c** ALBEDO. Units are m/s

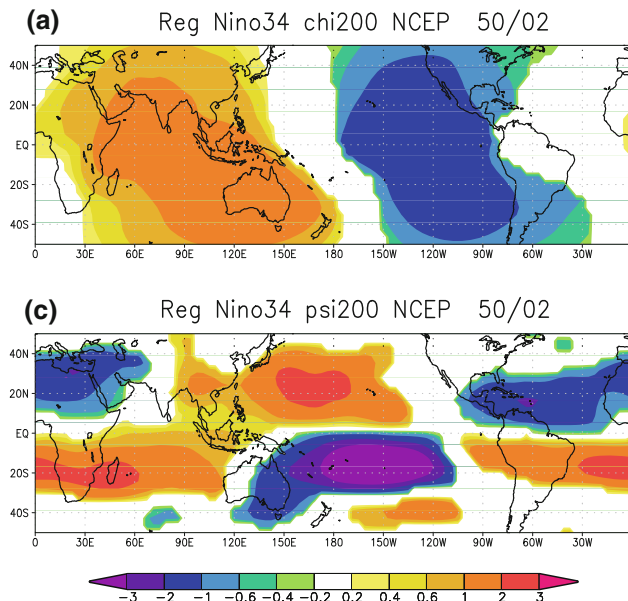


Fig. 12 Regressions onto the Nino34 index: **a** NCEP 200 hPa velocity potential, **b** C20C 200 hPa velocity potential, **c** NCEP 200 hPa eddy streamfunction, **d** C20C 200 hPa eddy streamfunction. Units are $10^6 \text{ m}^2/\text{s}$

found. The upper-level streamfunction response to a positive (negative) ENSO forcing is in quadrature with this, providing an eastward (westward) shift of the eddy streamfunction maximum. This leads to the hypothesis that part of the ENSO signal may be simply interpreted as due to a longitudinal shift of the streamfunction and velocity potential centres. This is partly confirmed by rainfall observations, which indeed display an east–west dipole signal as response to the ENSO forcing.

In all the idealized simulations presented in this paper, climatological SSTs have been imposed in the Indian Ocean region to force the ICTP AGCM. The Indian Ocean SSTs are characterized by a relatively broad warm pool (see Fig. 1). We find that the largest re-distribution of precipitation is between the regions of highest SST, one located in the Bay of Bengal, the other in the equatorial Indian Ocean (Fig. 8). The presence of these ITCZ-like precipitation centres is consistent with the argument of Chao and Chen (2001), and the east–west heating contrast controls the relative strength of the two centres. Prescribing zonally mean SSTs also in the Indian Ocean leads to a precipitation maximum at 8°N centered in the Indian Ocean (not shown), and if the east–west contrast is superimposed in this situation the precipitation pattern is only shifted northward by a few degrees. Thus the response of rainfall in the Indian basin to remote forcings depends on the mean state of the Indian Ocean.

Climate change projections of the mean state of the tropical Pacific are very uncertain: Most coupled climate models forecast an overall warming of few degrees in this region, but the patterns of such warming differ significantly

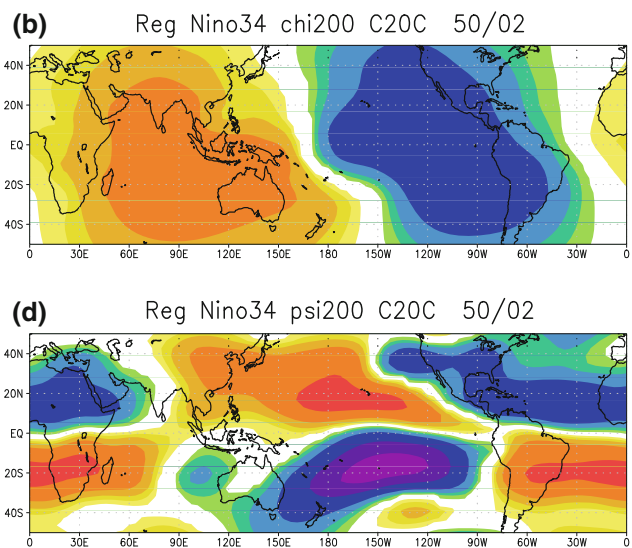


Fig. 13 Difference in regression onto the Nino34 index between NCEP and C20C models. **a** Reg Nino34 chi200 NCEP - C20C 50/02, **b** Reg Nino34 psi200 NCEP - C20C 50/02. Units are $10^6 \text{ m}^2/\text{s}$

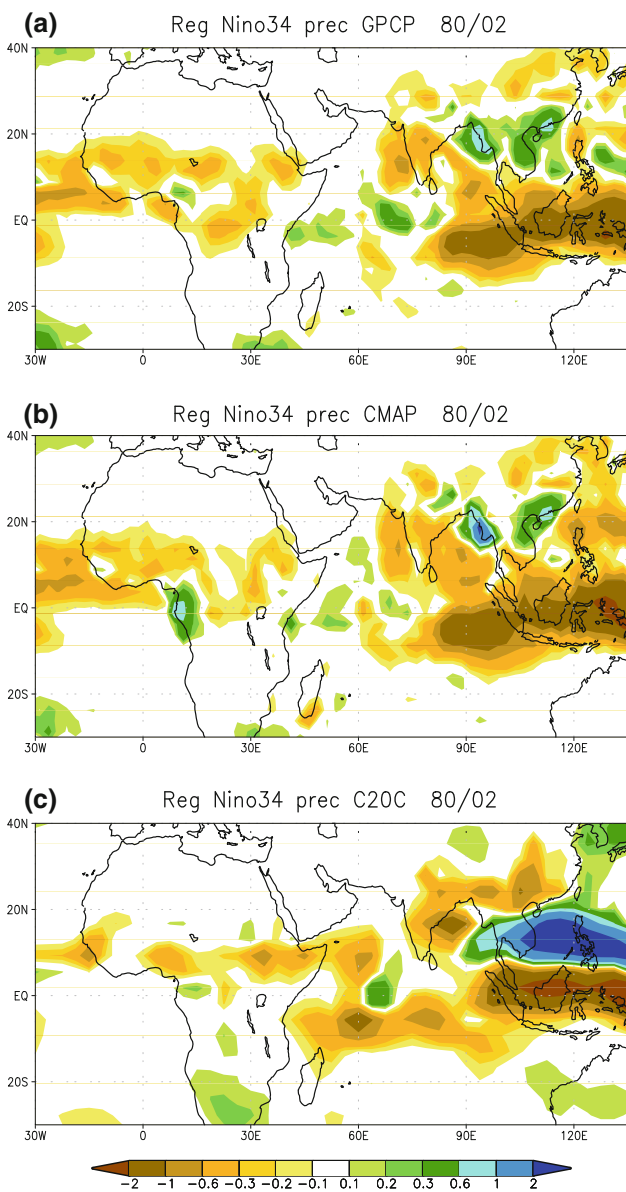


Fig. 13 Regressions of rainfall onto the Nino34 index: **a** GPCP, **b** CMAP, **c** C20C. Units are mm/day

from model to model (e.g. Lin 2007 and Collins et al. 2005). Our analysis shows that the details of the zonal temperature distribution are crucial to the South Asian monsoon system, and therefore have to be monitored with special care.

Acknowledgments The authors thank two anonymous reviewers for their constructive comments that helped improving the paper. The experiments described were performed as a contribution to the ENSEMBLES project funded by the European Commission Programme, contract number GOCE-CT-2003-505539 and as a contribution to the ‘International Climate of the 20th Century Project’ (C20C), coordinated by the Hadley Centre for Climate Prediction and Research (United Kingdom) and the Center for Ocean-Land-Atmosphere Studies (Calverton, Maryland).

References

- Adler RF, Huffman GL, Chang A et al (2003) The Version-2 Global Precipitation Climatology Project (GPCP) monthly precipitation analysis (1979–present). *J Hydrometeorol* 4(6):1147–1167
- Annamalai H, Hamilton K, Sperber KR (2007) The South Asian summer monsoon and its relationship with ENSO in the IPCC AR4 simulations. *J Clim* 20:1071–1092
- Boos WR, Kuang Z (2010) Dominant control of the South Asian monsoon by orographic insulation versus plateau heating. *Nature* 463:218–222
- Bourke W (1974) A multilevel spectral model. I. Formulation and hemispheric integrations. *Mon Wea Rev* 102:687–701
- Bracco A, Kucharski F, Kallummal R, Molteni F (2004) Internal variability, external forcing and climate trends in multi-decadal AGCM ensembles. *Clim Dyn* 23:659–678
- Bracco A, Kucharski F, Molteni F, Hazeleger W, Severijns C (2007) A recipe for simulating the interannual variability of the Asian Summer Monsoon and its relation with ENSO. *Climate Dyn* 28. doi:[10.1007/s00382-006-0190-0](https://doi.org/10.1007/s00382-006-0190-0)
- Chao WC, Chen B (2001) The origin of Monsoons. *J Atmos Sci* 58:3497–3507
- Chen T-C (2003) Maintenance of summer Monsoon circulations: a planetary perspective. *J Clim* 16:2022–2037
- Chou C (2003) Land–sea heating contrast in an idealized Asian summer monsoon. *Clim Dyn* 21:11–25
- Collins M, The CMIP modelling groups (2005) El Niño- or La Niña-like climate change?. *Clim Dyn* 25:89–104
- Folland CK, Shukla J, Kinter J, Rodwell MJ (2002) The climate of the Twentieth Century project. *CLIVAR Exch* 7(2):37–39
- Gill AE (1980) Some simple solutions for heat-induced tropical circulations. *Q J R Meteorol Soc* 106:447–462
- Goswami BN (1998) Interannual variations of Indian Summer Monsoon in a GCM: external conditions versus internal feedbacks. *J Clim* 11:501–521
- Held IM, Suarez MJ (1994) A proposal for the intercomparison of the dynamical cores of atmospheric general circulation models. *Bull Am Meteorol Soc* 75:1825–1830
- Holton JR (1992) Introduction to Dynamic Meteorology, 3rd edn. Academic Press, San Diego, p 511
- Ju J, Slingo JM (1995) The Asian Summer Monsoon and ENSO. *Q J R Meteorol Soc* 121:1133–1168
- Kalnay E, Kanamitsu M, Kistler R, Collins W, Deaven D, Gandin L, Iredell M, Saha S, White G, Woollen J, Zhu Y, Chelliah M, Ebisuzaki W, Higgins W, Janowiak J, Mo C, Ropelewski C, Wang J, Leetmaa A, Reynolds R, Jenne R, Joseph D (1996) The NCEP/NCAR 40-year reanalysis project. *Bull Am Meteorol Soc* 77:437–431
- Krishna Kumar K, Hoerling M, Rajagopalan B (2005) Advancing dynamical prediction of Indian monsoon rainfall. *Geophys Res Lett* 32:L08704. doi:[10.1029/2004GL021979](https://doi.org/10.1029/2004GL021979)
- Kucharski F, Molteni F, Bracco A (2006a) Decadal interactions between the Western Tropical Pacific and the North Atlantic Oscillation. *Clim Dyn* 26:79–91. doi:[10.1007/s00382-005-0085-5](https://doi.org/10.1007/s00382-005-0085-5)
- Kucharski F, Molteni F, Yoo JH (2006b) SST forcing of decadal Indian Monsoon rainfall variability. *Geophys Res Lett* 33:L03709. doi:[10.1002/2005GL025371](https://doi.org/10.1002/2005GL025371)
- Kucharski F, Bracco A, Yoo JH, Molteni F (2007) Low-frequency variability of the Indian Monsoon-ENSO relation and the Tropical Atlantic: The ‘weakening’ of the ‘80s and 90s. *J Clim* 20:4255–4266. doi:[10.1175/JCLI4254.1](https://doi.org/10.1175/JCLI4254.1)
- Kucharski F, Bracco A, Yoo JH, Molteni F (2008) Atlantic forced component of the Indian monsoon interannual variability. *Geophys Res Lett* 35:L04706. doi:[10.1029/2007GL033037](https://doi.org/10.1029/2007GL033037)

- Kucharski F, Bracco A, Yoo JH, Tompkins AM, Feudale L, Ruti P, Dell'Aquila A (2009a) A Gill-Matsun-type mechanism explains the Tropical Atlantic influence on African and Indian Monsoon rainfall. *Q J R Meteorol Soc* 135:569–579. doi:[10.1002/qj.406](https://doi.org/10.1002/qj.406)
- Kucharski F, Scaife A, Yoo JH et al (2009b) The CLIVAR C20C project: skill of simulating Indian monsoon rainfall on interannual to decadal timescales. Does GHG forcing play a role? *Clim Dyn* 33:615–627. doi:[10.1007/s00382-008-0462-y](https://doi.org/10.1007/s00382-008-0462-y)
- Li C-F, Yanai M (1996) The onset and interannual variability of the Asian summer monsoon in relation to land–sea thermal contrast. *J Clim* 9:358–375
- Li Y, Lu R, Dong B (2007) The ENSO-Asian Monsoon interaction in a coupled Ocean–Atmosphere GCM. *J Clim* 20:5164–5177. doi:[10.1175/JCLI4289.1](https://doi.org/10.1175/JCLI4289.1)
- Lin J (2007) The Double-ITCZ problem in IPCC AR4 coupled GCMs: Ocean Atmosphere feedback analysis. *J Clim* 20:4497–4525
- Losada T, Rodriguez-Fonseca B, Polo I, Janicot S, Gervois S, Chauvin F, Ruti P (2009) Tropical response to the Atlantic Equatorial mode: AGCM multimodel approach. *Clim Dyn.* doi:[10.1007/s00382-009-0624-6](https://doi.org/10.1007/s00382-009-0624-6)
- Meehl GA (1994) Influence of the land surface in the Asian summer monsoon: External conditions versus internal feedbacks. *J Clim* 7:1033–1049
- Molteni F (2003) Atmospheric simulations using a GCM with simplified physical parametrizations. I: model climatology and variability in multi-decadal experiments. *Clim Dyn* 20:175–191
- Rasmusson EM, Carpenter TH (1983) The relationship between the eastern Pacific sea surface temperature and rainfall over India and Sri Lanka. *Mon Weather Rev* 111:517–528
- Rayner NA, Parker DE, Horton EB, Folland CK, Alexander LV, Rowell DP, Kent EC, Kaplan A (2003) Global analyses of SST, sea ice, and night marine air temperature since the late nineteenth century. *J Geophys Res* 108(D14). doi:[10.1029/2002JD002670](https://doi.org/10.1029/2002JD002670)
- Rodwell MJ, Hoskins BJ (2001) Subtropical Anticyclones and Summer Monsoons. *J Clim* 14:3192–3211
- Scaife AA, Kucharski F, Folland CK, Kinter J, Brönnimann S, Fereday D, Fischer AM, Grainger S, Jin EK, Kang IS, Knight JR, Kusunoki S, Lau NC, Nath MJ, Nakaegawa T, Pegion P, Schubert S, Sporyshev P, Syktus J, Yoon JH, Zeng N, Zhou T (2009) The CLIVAR C20C project: selected twentieth century climate events. *Clim Dyn* 33:603–614
- Turner AG, Inness PM, Slingo JM (2005) The role of the basic state in the monsoon-ENSO relationship and implications for predictability. *Q J R Meteorol Soc* 131:781–804
- Turner AG, Inness PM, Slingo JM (2007) The effect of doubled CO₂ and model basic state biases on the monsoon-ENSO system. I: mean response and interannual variability. *Q J R Meteorol Soc* 133:1143–1157
- Walker GT (1924) Correlations in seasonal variations of weather. *Mem Ind Meteorol Dept* 24:275–332
- Wallace JM, Hobbs PV (1977) Atmospheric Science: An introductory Survey. Academic Press, London, 467 p
- Wang B, Ding Q, Fu X, Kang I-S, Jin K, Shukla J, Doblas-Reyes F (2005) Fundamental challenge in simulation and prediction of summer monsoon rainfall. *Geophys Res Lett* 32. doi:[10.1029/2005GL022734](https://doi.org/10.1029/2005GL022734)
- Wang B (2006) The Asian Monsoon. Springer, Berlin, ISBN 3-540-40510-7, 638 p
- Webster PJ (1987) The Elementary Monsoon. In: Fein JS, Stephens PL (eds) *Monsoons*, Wiley, London, p 3–32
- Webster PJ, Yang S (1992) Monsoon and ENSO: Selectively interactive systems. *Q J R Meteorol Soc* 118:877–926
- Wu R, Kirtman BP (2005) Roles of Indian and Pacific Ocean air-sea coupling in tropical atmospheric variability. *Clim Dyn* 25:155–170
- Xie P, Arkin PA (1997) Global precipitation: a 17-year monthly analysis based on gauge observations, satellite estimates and numerical model outputs. *Bull Am Meteorol Soc* 78:2539–2558